

# Influence of the temperature on the charge transport and recombination profile in organic bulk heterojunction solar cells: a drift-diffusion study

Ali Mahmoudloo<sup>1</sup> · Sohrab Ahmadi-Kandjani<sup>1</sup>

Received: 9 January 2015 / Accepted: 23 March 2015 / Published online: 29 March 2015  
© Springer-Verlag Berlin Heidelberg 2015

**Abstract** Charge transport and recombination in organic semiconductors in the presence of temperature have an important role in device efficiency. In this study, we investigated the influence of the temperature on the charge transport and charge carrier generation and recombination kinetics in bulk heterojunction solar cells based on poly(3-hexylthiophene) (P3HT) and a methanofullerene derivative (PCBM). By solving the drift diffusion and Poisson equations via finite element method, the effects of the temperature on characteristic parameters of the cell have been studied. Considering the effect of different recombination models such as Langevin, trap-assisted and geminate recombinations, at low temperature of cell a reduction in the recombination rate observed, and therefore, open-circuit voltage ( $V_{oc}$ ) increased by decreasing the temperature. Langevin recombination is a dominating factor in total recombination which geminate recombination has very little impact on the total recombination rate. It was shown that  $V_{oc}$  is mainly governed by the dynamics of the charge transfer state and it significantly affected by carrier recombination profile. Detail study of the exciton profile and influences on the  $V_{oc}$  will allow for a more efficient donor/acceptor cell design, which can be led to improve photovoltaic performance. Calculated  $J$ – $V$  characteristics and temperature dependence of  $V_{oc}$  reveal relatively good agreement between the model's predictions and published modeling and experimental reports.

## 1 Introduction

In recent years, due to unusual mechanical and photo-physical properties of organic semiconductor materials, there have been tremendous interests in developing a variety of innovative modern electronic and optoelectronic devices, such as organic light-emitting diodes (OLED), organic solar cells (OSC) and organic field effect transistors [1–4]. Efficient and low-cost production, physical flexibility and non-toxic property of organic semiconductors make them a good alternative to common inorganic semiconductors [5–7]. On the other hand, because of the mentioned aspects and also near infrared light absorption and red–green–blue emission characteristics, organic semiconductors are much desired candidates in solar cells and also fluorescent and phosphorescent OLEDs [8–10].

It has been shown that important characteristics of OSC (OPVs) highly depend on both fabrication methods and also cell working conditions. In addition to experimental studies, numerical device modeling methods provide a good understanding and efficient optimization for designing organic optoelectronics devices [11–13]. Schematic energy-level diagrams of the PEDOT:PSS/P3HT:PCBM/Al bulk heterojunction (BHJ) solar cell with the electrode materials are shown in Fig. 1. In this figure, highest occupied molecular orbital (HOMO) and lowest unoccupied molecular orbital (LUMO) levels, active region and energy diagram in applied voltage ( $V$ ) have been depicted. In the study of BHJ solar cells, device performance strongly depends on charge transport mechanisms which are affected by terrestrial conditions such as sunlight illumination, working temperature and also physical parameters such as the thickness of the active region, fabrication techniques, materials used, and encapsulation [13, 14]. Of special interest in this context is the charge transfer (CT) states that determine both the

✉ Ali Mahmoudloo  
mahmodlo@tabrizu.ac.ir

<sup>1</sup> Research Institute for Applied Physics and Astronomy (RIAPA), University of Tabriz, Tabriz, Iran

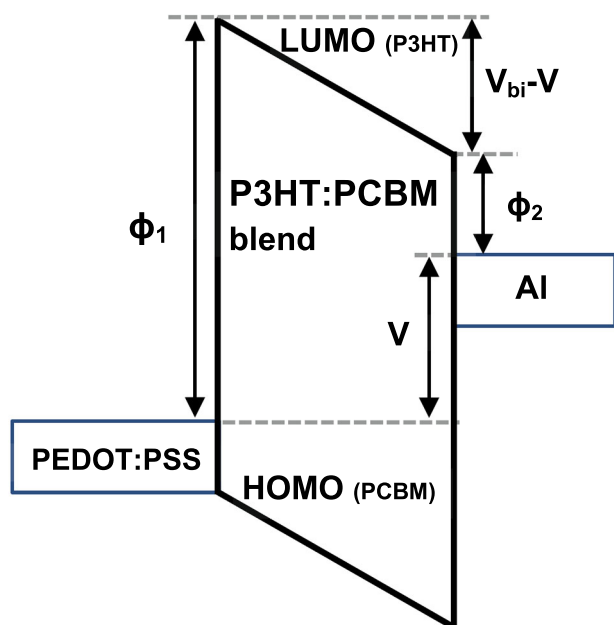


**Fig. 1** Schematic diagrams of the P3HT:PCBM BHJs OSC

transport properties of the material and the exciton dissociation and recombination rates that influence electroluminescent and photovoltaic efficiencies [15, 16]. Following the impressive developments in designing efficient organic photovoltaic cells, internal quantum efficiency of P3HT:PCBM based OPVs has reached 100 % [2, 3], implying that energy conversion efficiency is most likely limited by open-circuit voltage ( $V_{oc}$ ), low fill factor and insufficient/narrow absorption [17–19].  $V_{oc}$  depends on device bandgap which is related to the HOMO of electron donating (donor) and the LUMO of the electron withdrawing (acceptor) materials, temperature, density of states and charge carrier density. Further,  $V_{oc}$  is rather complex due to the temperature dependence of both hole and electron charge carrier density, bandgap, etc. Additionally,  $V_{oc}$  is known to be related to the fundamental thermodynamic parameters such as the statistics of occupancy of transport and trap states [20]. An exact interpretation of the  $V_{oc}$  dependence on temperature may be carried out by numerical simulation. Thus, to find high-efficiency cell with high  $V_{oc}$ , it is so important to investigate the detailed phenomena of charge carrier transport, charge carrier generation and recombination in polymer:fullerene BHJ solar cells. In addition, drift-diffusion modeling of OPVs has been demonstrated to be a powerful tool to explain the influence of various effects on the device performance, and beside the experimental results, these simulations can be employed predictively to define requirements of desired material properties [21].

In this paper, we investigated the influence of the temperature on the charge carrier transport and recombination

processes in polymer:fullerene BHJ solar cell device. In our study, we have chosen a temperature range from  $-10$  to  $50$  °C which is the typical terrestrial temperature range of the earth. In particular, in this model, by solving self-consistent drift diffusion and Poisson equations via finite element method (FEM) and also considering the boundary condition, solar cell characteristics such as carriers density, recombination rates and  $V_{oc}$  in different temperature at optimum device thickness (100 nm) have been calculated. In OPVs, charge recombination processes are those in which spatially separated charges combine to form localized excited states [22]. Considering the effect of different recombination models such as bimolecular or Langevin recombination, Shockley–Read–Hall (SRH) recombination or trap-assisted and geminate recombinations,  $V_{oc}$  is mainly governed by the dynamics of the CT state and it significantly affected by recombination profile. In the present study, we look closely at temperature effects on exciton generation and recombination and temperature influences on  $V_{oc}$  that these effects play an important role in performance of the OSC device. Simulated current–voltage ( $J$ – $V$ ) characteristics and temperature dependence of  $V_{oc}$  reveal relatively good agreement between the model’s predictions and published modeling and experimental reports [18, 19].

## 2 Models and methods

In any types of solar cells,  $V_{oc}$  is depended on the bandgap,  $E_g$ , which in the case of the OPVs moreover it is related to the  $E_g = E_{LUMO}(A) - E_{HOMO}(D)$  [23], and also it is dependent upon a number of physical parameters, such as sunlight illumination intensity, working temperature, the quality of the anode and cathode contacts, charge carrier mobilities, exciton generation and recombination rates. So, it is so important to study the detailed recombination processes for understanding of origin and nature of  $V_{oc}$ . Generally, there are three types of recombinations that cause losses in bulk heterojunction solar cells:

### 2.1 Bimolecular or Langevin recombination

Bimolecular or Langevin recombination,  $R_0$ , with the recombination constant  $\beta$  and the intrinsic charge carrier density  $n_i$  that governed by electron ( $n$ ) and hole ( $p$ ) density is given by the following equation:

$$R_0 = \beta(np - n_i^2), \quad (1)$$

which Langevin theory gives a description of  $\beta$  as a function of mobilities of electron and hole,  $\mu_n$  and  $\mu_p$ , respectively:

$$\beta = q \frac{(\mu_n + \mu_p)}{\varepsilon\varepsilon_0}, \tag{2}$$

In this equation,  $\varepsilon\varepsilon_0$  is the permittivity of the active layer material,  $q$  is the elementary charge and  $\mu_n$  and  $\mu_p$  are electron and hole mobility, respectively. For the pristine materials, charge carriers both belong to the same material and could move in all directions, while the recombination occurs in a point near to the charge carrier having low mobility [24]. On the other hand, in the organic BHJ solar cells, the electron and hole belong to two different matters and the recombination happens in the interface between two different matters. A charge carrier having more mobility reaches the interface sooner, but it should wait a little more until the charge carrier with low mobility reaches the interface. Hence, in the blend matter, the charge carrier that having low mobility determines the recombination conditions. In our simulation, we assume that carriers' mobility is equal.

### 2.2 Geminate recombination or recombination via CT state

Free charge carrier generation in this type of recombination is explained using the geminate recombination theory presented by Onsager [25, 26]. This theory was later developed by Braun considering the hole–electron pair as a precursor to the free charge carriers with limited lifetimes [26]. In this type of recombination, the bound electron–hole pair with binding energy  $E_B$  is regarded as an intermediate state where the recombination and dissociation of charge carriers are performed through this intermediate phase.

EB is considered as an intermediate state where the recombination and dissociation of charge carriers are triggered through this intermediate state. It is possible for the electron–hole pair to return to the initial state or dissociated to the free charge carriers. This charge carrier dissociation is a competition between the separation rate,  $k_{diss}$ , and the recombination of charge carriers that is conducted through an intermediate phase or the CT state. In Braun's model, the electron–hole dissociation probability is given as the following equation:

$$p(x, T, F) = \frac{k_{diss}(x, T, F)}{k_{diss}(x, T, F) + k_f(T)}, \tag{3}$$

Here,  $x$  is the distance between the electron and hole,  $F$  is the power of the field and  $T$  is the temperature. The decay rate of the bound electron–hole pair to the ground state,  $k_f$ , is used as a fit parameter. As polymer systems are subject to disorder, it is reasonable to assume that the electron–hole pair distance is not constant throughout the system [15, 27], where  $k_{diss}$  follows the following equation:

$$k_{diss}(x, T, F) = \beta \exp\left(\frac{-E_B}{K_B T}\right) f(E, E_0), \tag{4}$$

As a result, Eq. 3 should be integrated over a distribution of separation distances

$$P(x, T, F) = \int_0^\infty p(x, T, F) f(a, x) dx, \tag{5}$$

where  $f(a, x)$  is a normalized distribution function given by [28]

$$f(a, x) = \frac{4}{\sqrt{\pi} a^3} x^2 \exp(-x^2/a^2), \tag{6}$$

This leads to a modification of free charge carrier recombination terms by  $P$ , which describes the probability of the dissociation of a CT state, and consequently geminate recombination determined as [21, 27],

$$R_{geminate} = R_{lang}(1 - P), \tag{7}$$

### 2.3 Trap-assisted recombination

Another mechanism resulting a loss in the OSC is the indirect recombination. To calculate the type of recombination, we take into account the trap-assisted Shockley–Read–Hall with the trap density  $N_t$  and the capture coefficient  $C_t$  [29, 30].

$$R_{SRH} = C_t N_t \frac{np - n_i^2}{n + p + n_d + p_0}, \tag{8}$$

which  $n_d$  and  $p_0$  are characteristic charge carrier densities. For the sake of simplicity, we assume a temperature-independent effective bandgap.

### 2.4 The model

The electrical behavior of OPVs can be estimated by a numerical model based on simultaneous solving coupled self-consistent current continuity and Poisson equations. Poisson equation is:

$$\frac{d}{dx} E(x) = \frac{q}{\varepsilon_r \varepsilon_0} (p(x) - n(x)), \tag{9}$$

where  $E$  is applied electric field. This equation correlates the electrons and holes mobilities to spatial variations of the electric field. The current density continuity equations for electrons and holes are:

$$\begin{aligned} J_n(x) &= \mu_n n(x) E(x) + D_n \frac{d}{dx} n(x) \\ J_p(x) &= \mu_p p(x) E(x) - D_p \frac{d}{dx} p(x), \end{aligned} \tag{10}$$

In these equations,  $J_n$ ,  $J_p$ ,  $D_n$  and  $D_p$  are electron current density, hole current density, and diffusion coefficients of electrons and holes, respectively. The charge concentration continuity equations for electrons and holes are:

$$\begin{aligned} \frac{d}{dt}n(x) &= \frac{1}{q} \frac{d}{dx} J_n(x) + G(x) - R(x) \\ \frac{d}{dt}p(x) &= \frac{1}{q} \frac{d}{dx} J_p(x) + G(x) - R(x), \end{aligned} \quad (11)$$

where  $G$  is the generation rate of free charge carrier result in the separation of exciton and  $R$  is total recombination rate of charge carriers that it is sum of three Langevin, SRH and geminate recombinations [30]. Meaning the total produced charge carriers are recombined inside the bulk, and hence, we ignore the current gradient. In our study, we solve these equations via FEM by applying the boundary conditions and 100 nm active layer thickness. Finally, by calculating the charge continuity equations, it is possible to calculate  $J_{sc}$ ,  $V_{oc}$ , FF, cell efficiency and  $J$ - $V$  characteristics in different doping concentration. The calculation of the  $\eta$  has been done using the equation:

$$\eta = \frac{J_{sc} V_{oc} FF}{P_{in}}, \quad (12)$$

where  $P_{in}$  is the incident light power. The FF measures the quality of the solar cell as a power source and is defined as the ratio between the maximum power delivered to an external circuit and the potential power according to:

$$FF = \frac{J_{max} V_{max}}{J_{sc} V_{oc}}, \quad (13)$$

where  $J_{max}$  and  $V_{max}$  are the values of the voltage and current density for maximizing their product of the  $JV$  curve in the fourth quadrant, where the device operates as an electrical power source. Assuming Gaussian DOS of both the HOMO and LUMO levels,  $V_{oc}$  is defined as the quasi-Fermi level splitting the solar cell can reach under illumination without load:

$$qV_{oc} \sim E_g - k_B T \ln \left( \frac{q}{N_c N_v} (pn) \right), \quad (14)$$

This equation shows that the key expression to understand the dependence of  $V_{oc}$  on recombination is given by  $n$  and  $p$ , which exact interpretation of the  $V_{oc}$  dependence on temperature may be calculated self-consistently in the numerical simulation. The temperature dependence of Eq. 14 might be rather complex. In addition to the explicit dependencies on  $T$ ,  $n$  and  $p$  also vary with temperature. Charge carrier densities in the cell will be determined by the generation–recombination of kinetic balance under constant illumination. Thus, in this work we investigate effects of temperature on carrier density, carrier recombination and  $V_{oc}$  via numerical simulation.

### 3 Results and discussion

The most exciting trend is that all the curves are at different temperatures, and active region thickness has been chosen 100 nm. It has been demonstrated that absorption of the blend remains constant between 80 and 320 K [18]. For this reason, we assume that  $J_{sc}$  is constant that in our calculations it has been shown that generation rate is constant which these results are in good agreement with experimental results in other literature [18]. In fact,  $J_{sc}$  is constant as temperature is reduced to a certain critical temperature (TC) for particular intensities. TC in 1.5 AM sunlight illumination is about 230 K, and above this TC, same as our study, it demonstrates that the generation rate is constant [18]. All parameters used in our numerical simulation are given in Table. 1.

Figure 2a, b shows the Langevin, SRH, geminate and total recombination rate profile in  $-10^\circ\text{C}$  and  $50^\circ\text{C}$  in terms of distance from anode. As shown in the figure, near the contacts, recombination rates are too low. Since the charge carrier densities near the contacts are low, recombination of carriers is weak and hence the recombination lifetime of the charge carriers is relatively long. In fact, due to the high field strength, the charge carriers needed time to exit from the active layer region is too small, and therefore only few charge carriers are lost due to the recombination. In both Fig. 2a, b, bimolecular or Langevin recombination is a dominating factor and geminate recombination is very little impact on the total recombination rate. In the case of a higher temperatures, Fig. 2b, the minority charge carriers tend to move toward the middle of the device to reach their densities close to the contact, and as shown in the figure, the recombination maximum is found in the center of the device. But by decreasing the temperatures (Fig.2a), charge carrier density decreases and also charge carrier transport is slower than the recombination process and charge carriers

**Table 1** Parameters that used in numerical simulation

Parameter	Symbol	Value
Active layer thickness	P3HT:PCBM	100 nm
Temperature	$T$	Vary $C$
Bandgap	$E_g$	1.8 eV
Electron mobility	$\mu_e$	$2 \times 10^{-5} \text{ cm}^2/\text{Vs}$
Hole mobility	$\mu_h$	$2 \times 10^{-4} \text{ cm}^2/\text{Vs}$
Recombination constant	$\beta$	$1.95 \times 10^{-12} \text{ -}$
Dielectric constant	$\varepsilon(\varepsilon_0)$	$3.36 \times 10^{-11} \text{ F/cm}$
Effective density of states	$N_c, N_v$	$1.4 \times 10^{18} \text{ cm}^{-3}$
Doping levels	$n_d, p_0$	$10^{19} \text{ cm}^{-3}$
Incident sunlight power	$P_{in}$	$840 \text{ Wm}^{-2}$

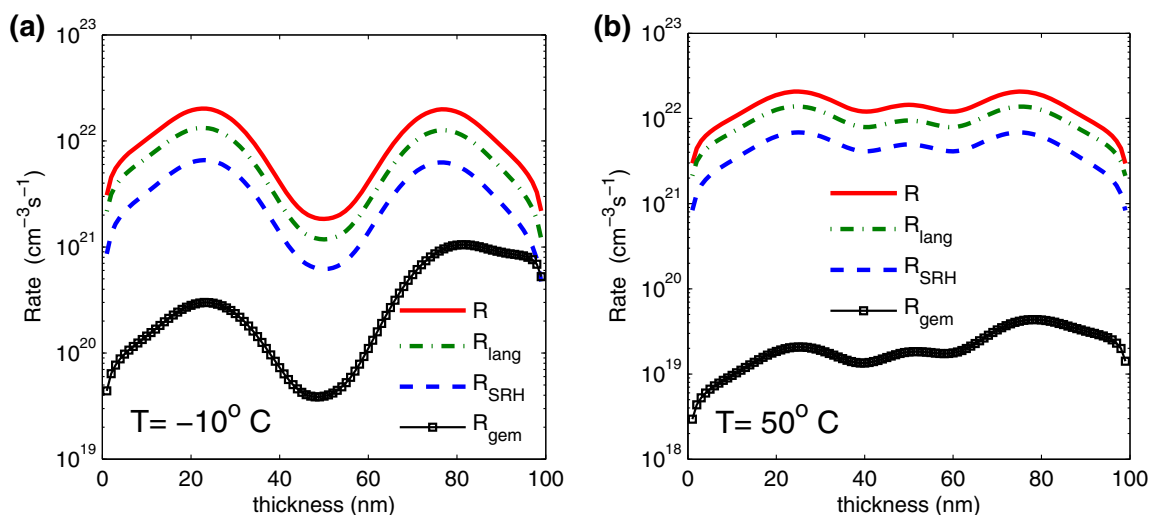


**Fig. 2** Langevin, SRH, geminate and total recombination rate profile in (a)  $-10^{\circ}\text{C}$  and (b)  $50^{\circ}\text{C}$  in terms of distance from anode

recombine mainly close to the contacts where they are created by absorbing the light.

For a good comparison with how temperature affects the recombination profile, variation of the slope of recombination in terms of the different temperature can be shown in Fig. 3. This figure clearly shows that by increasing temperature, how recombination in middle of the cell increases and in  $50^{\circ}\text{C}$  reached to maximum value. Thus, at high temperatures, carriers recombine before reaching to the contacts. When an electron–hole pair is formed by absorbing light, electrons have three destinations; first, they accumulate in cathode, second, they are recombined with the hole, and third, they go to anode and accumulate in there. Electrons could recombine with the holes produced by light as well as holes coming from anode with high work function. Figure 4a, b demonstrates the distribution density profile of electrons, holes and generation and recombination rate in two different temperatures ( $-10$  and

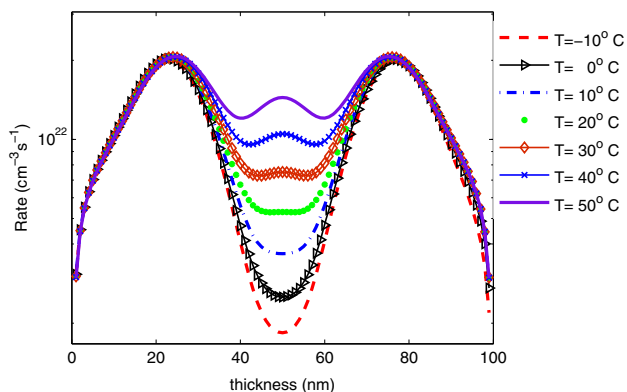


**Fig. 3** Total recombination rate profile in different temperatures in terms of distance from anode

$50^{\circ}\text{C}$ ) in terms of distance from anode. As shown in the figure, low loss of charge carriers close to the contacts is a consequence of the high field strength, which ensures good charge extraction, resulting in low carrier densities at device structure, because the density of charge carriers will decrease with decreasing the temperature, and this results in the reduction in recombination; thus, this effect makes the efficiency of the system to rise. As shown in Fig. 4, at high-temperature condition ( $50^{\circ}\text{C}$ ), more charge carriers transfer to the entire of the device in comparison with the case of  $-10^{\circ}\text{C}$ , so this accumulation of charge carriers will cause increase recombination inside the bulk in  $50^{\circ}\text{C}$ , and it is expected that it will thereby reducing the system efficiency. As the temperature decreases, the density of charge carriers inside the sample will decrease. Therefore, the density of electrons and holes is higher near the electrodes than in other places inside the bulk. This issue is clearly shown in Fig. 4.

Figure 5 shows the  $J$ – $V$  characteristics for polymer:fullerene OPV in different temperatures. As denoted,  $J_{sc}$  is constant as TC higher than 230 K, so in the case of our study which temperature chosen above 263 K, with a good assumption we can use constant  $J_{sc}$  in our calculation [18]. As shown in the figure, by increasing the temperature,  $V_{oc}$  decreases. In fact, the maximum attainable  $V_{oc}$  achieved at 0 K for a donor–acceptor combination [31, 32]. Under illumination,  $V_{oc}$  is related to the splitting of quasi-Fermi levels, which depend on the charge carrier densities in the LUMO and HOMO density of states [33]. In a steady state,  $G$  and  $R$  are in equilibrium, which set the charge carrier densities [33, 34]. One expressing  $V_{oc}$  governed by free charge carrier concentrations and lifetimes that are related to and the other correlating the CT-state energy with  $V_{oc}$  in theory and experiment [35, 36]. Figure 6 shows the

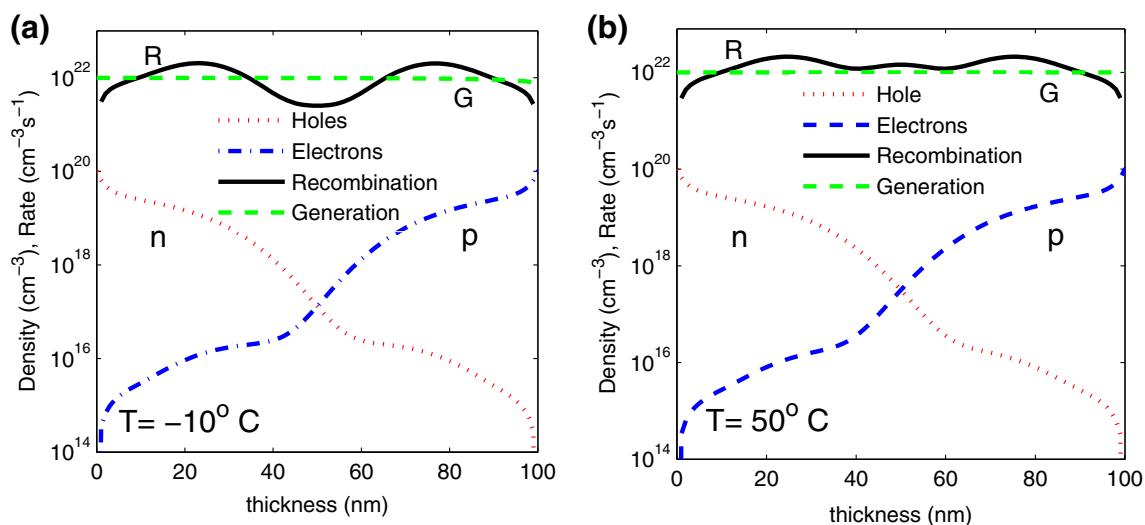


**Fig. 4** Distribution density profile of electrons, holes and generation and recombination rate in (a)  $-10\text{ }^{\circ}\text{C}$  and (b)  $50\text{ }^{\circ}\text{C}$  in terms of distance from anode

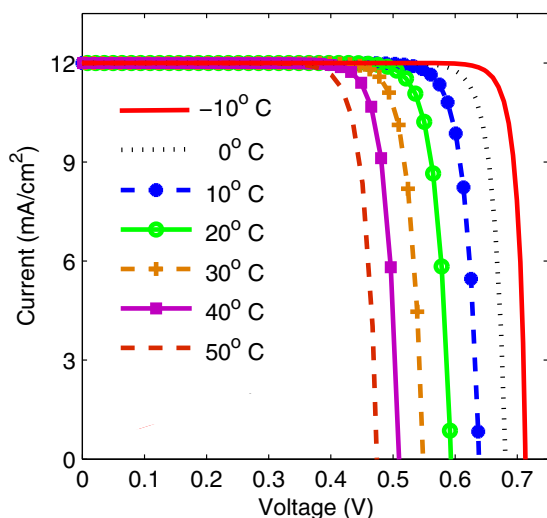


**Fig. 5**  $J$ - $V$  characteristics for polymer:fullerene OPV in different temperatures

variation of  $V_{oc}$  with respect to temperature. As shown in the figure, variation of the  $V_{oc}$  versus temperature is a linear relation, so as the temperature increases,  $V_{oc}$  decreased linearly.

#### 4 Conclusion

In this study, we have studied the temperature-dependent characteristics of polymer:fullerene-based organic BHJ solar cells. By considering the different recombination models such as Langevin, SRH or trap-assisted and geminate recombinations, the effects of the temperature on cell characteristic parameters have been studied. It was shown

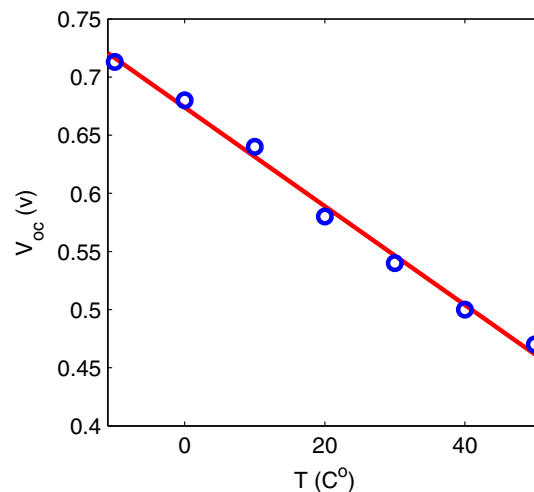


**Fig. 6** Variation of the  $V_{oc}$  for polymer:fullerene OPV in different temperatures

that minority charge carriers tend to move toward the middle of the device to reach their densities close to the contact and the maximum recombination rate is found in the center of the device at higher temperatures. Although in lower temperature charge carriers continue to recombine together entire the cell, recombination profile has very different form and charge carriers recombine mainly close to the contacts where they are generated. From the results, it was found that  $V_{oc}$  is mainly governed by the dynamics of the CT state and it significantly affected by Langevin recombination profile. Results clearly show a reduced recombination in the high-efficiency solar cells occurred by decreasing the temperature in polymer:fullerene mixtures. Calculated  $J$ - $V$  characteristics and temperature dependence

of  $V_{oc}$  reveal relatively good agreement between the model's predictions and published modeling and experimental reports.

## References

- N.S. Sariciftci, L. Smilowitz, A.J. Heeger, F. Wudl, *Science* **258**, 1474 (1992)
- C.J. Brabec, N.S. Sariciftci, J.C. Hummelen, *Adv. Funct. Mater.* **11**, 15 (2001)
- F.C. Krebs, *Sol. Energy Mater. Sol. Cells* **93**, 394 (2009)
- S. Hameed, P. Predeep, M.R. Baiju, *Rev. Adv. Mater. Sci.* **26**, 30 (2010)
- P.K.H. Ho, D. Stephen, R.H. Friend, N. Tessler, *Science* **285**, 233–236 (1999)
- M.K. Wei, C.W. Lin, C.C. Yang, Y.W. Kiang, J.H. Lee, H.Y. Lin, *Int. J. Mol. Sci.* **11**, 1527–1545 (2010)
- S. Kappaun, C. Slugovc, E.J.W. List, *Int. J. Mol. Sci.* **9**, 1527–1547 (2008)
- T. Tromholt, M. Manceau, M. Helgesen, J.E. Carle, F.C. Krebs, *Sol. Energy Mater. Sol. Cells* **95**, 1308 (2011)
- Y. Zhou, J. Pei, Q. Dong, X. Sun, Y. Liu, W. Tian, *J. Phys. Chem. C* **113**, 7882 (2009)
- H. Movla, A. Shahalizad, A.R. Nezamabad, *J. Opt. Quantum Electr.* **47**, 621–632 (2014)
- P. Schilinsky, C. Waldauf, J. Hauch, C.J. Brabec, *J. Appl. Phys.* **95**, 2816 (2004)
- B. Ruhstaller, T. Beierlein, H. Riel, S. Karg, J.C. Scott, W. Riess, *IEEE J. Sel. Top. Quantum Electron.* **9**, 723 (2003)
- J.D. Kotlarski, P.W.M. Blom, L.J.A. Koster, M. Lenes, L.H. Sloof, *J. Appl. Phys.* **103**, 084502 (2008)
- T. Kirchartz, T. Agostinelli, M.C. Quiles, W. Gong, J. Nelson, *J. Phys. Chem. Lett.* **3**, 3470 (2012)
- Y. Roichmann, N. Tessler, *Appl. Phys. Lett.* **80**, 1948 (2002)
- N. Tessler, Y. Preezant, N. Rappaport, Y. Roichman, *Adv. Mater.* **21**, 2741–2761 (2009)
- M. Kemerink, J.M. Kramer, H.H.P. Gommans, E.A.J. Janssen, *Appl. Phys. Lett.* **88**, 192108-3 (2006)
- A.K. Thakur, G. Wantz, G. Garcia-Belmonte, J. Bisquert, L. Hirsch, *Sol. Energy Mater. Sol. Cells* **95**, 2131–2135 (2011)
- G. Garcia-Belmonte, *Sol. Energy. Sol. Cells* **94**, 2166–2169 (2010)
- G. Garcia-Belmonte, P.P. Boix, J. Bisquert, M. Sessolo, H.J. Bolink, *Sol. Energy Mater. Sol. Cells* **94**, 366–375 (2010)
- W. Tress, K. Leo, M. Riede, *Phys. Rev. B* **85**, 155201-11 (2012)
- J. Kalinowski, M. Cocchi, P. Di Marco, W. Stampor, G. Giro, V. Fattori, *J. Phys. D.* **33**, 2379–2387 (2000)
- J. Bisquert, D. Cahen, G. Hodes, S. Ruhle, A. Zaban, *J. Phys. Chem. B* **108**, 8106–8118 (2004)
- J.J.M. Halls, C.A. Walsh, N.C. Greenham, E.A. Marseglia, R.H. Friend, S.C. Moratti, A.B. Holmes, *Nature* **376**, 498–500 (2002)
- L. Onsager, *Phys. Rev.* **54**, 554-7 (1938)
- C.L. Braun, *J. Chem. Phys.* **80**, 4157 (1984)
- L.J.A. Koster, E.C.P. Smits, V.D. Mihailetschi, P.W.M. Blom, *Phys. Rev. B* **72**, 085205-9 (2005)
- V.D. Mihailetschi, L.J.A. Koster, J.C. Hummelen, P.W.M. Blom, *Phys. Rev. Lett.* **93**, 216601-4 (2004)
- W. Shockley, W.T. Read Jr, *Phys. Rev.* **87**, 835 (1952)
- S.M. Sze, *Phys. Semicond. Devices*, 2nd edn. (Wiley, USA, 2005)
- R. Hamilton, C.G. Shuttle, B. O'Regan, T. Hammant, J. Nelson, J.R. Durrant, *J. Phys. Chem. Lett.* **1**, 1432–1436 (2010)
- A. Foertig, A. Baumann, D. Rauh, V. Dyakonov, C. Deibel, *Appl. Phys. Lett.* **95**, 052104-3 (2009)
- M. Riede, T. Mueller, W. Tress, R. Schueppel, K. Leo, *Nanotechnology* **19**, 424001-12 (2008)
- G. Garcia-Belmonte, J. Bisquert, *Appl. Phys. Lett.* **96**, 113301-3 (2010)
- A. Maurano, R. Hamilton, C.G. Shuttle, A.M. Ballantyne, J. Nelson, B. O'Regan, W. Zhang, I. McCulloch, H. Azimi, M. Morana, C.J. Brabec, *Adv. Mater.* **22**, 4987 (2010)
- K. Vandewal, K. Tvingstedt, A. Gadisa, O. Inganas, J.V. Manca, *Phys. Rev. B* **81**, 125204 (2010)